JOURNAL OF APPLIED POLYMER SCIENCE VOL. VI, ISSUE NO. 22, PAGES 373-392 (1962)

A Study of the Compression Fatigue and the Damping Phenomena of Tire Cord

GÜNTER KEMMNITZ

Glanzstoff-Courtaulds. G.m.b.H., Cologne, Weidenpesch, Germany

In evaluating the dynamical characteristics of cords, impact resistance and adhesion as well as fatigue life and physical properties like creep, heat evolution, inflexibility, and damping are considered.

Numerous testing methods have been developed for this purpose. In the following the results obtained with the De Mattia method on bending and compression fatigue are discussed. Further tests on growth and damping under dynamic reciprocating tensile strength are evaluated.

The results of both testing procedures are compared with one another and with the performance of the cord in the tire.

1. Investigations of the Compression Fatigue of Tire Cords by the De Mattia Method

Tire producers and tire yarn manufacturers alike are interested in laboratory methods of testing the dynamic properties of cords. The performance of cords and tire fabrics is to be examined to ensure a control of the tire production and check variations in properties rising therefrom. On the other hand, these tests should enable the yarn producer to develop appropriate cord properties by varying the spinning process.

In spite of their importance, the dynamic testing methods have not been standardized so far. The reason for this may be the existence of many special methods, only a few of which provide results that correspond to the actual driving performance of the tire. The fact that an American firm has installed apparatus for more than a hundred testing methods according to each customer's request illustrates the difficulties still existing.

In 1953 Pieper[1] gave a summary of the apparently most important testing methods. In addition to the testing procedures described by Fromandi[2] on bending, flexing, abrasion, and impact fatigue of raw cords, he especially stressed the importance of the Goodrich Disk, Firestone, Mallory, and Pulser test developed by Schrode, the last one concerning rubber-imbedded cords. The compression fatigue tests of the rubber-textile compound can be considered an improvement over the raw cord tests in spite of added difficulties, since the cord is subjected to conditions similar to those occurring in the innermost plies of the tire.

Quite a few other methods, for instance the belt test developed by Illingworth,[3] could be mentioned here without giving a complete enumeration.

1.1 Description and Application of the De Mattia Method

In 1954 Kern[4] described the De Mattia or "flat pad" method for testing the compression fatigue of in-rubber cords. At present, this among similar methods is employed by several tire producers and will be adopted by other firms before long. This applies likewise to manufacturers of chemical fibers and tires.

The influence of various factors, such as flex angle, twist, testing frequency, and temperature, denier, dip, and cord types, on the compression fatigue have been investigated by means of this method, which should provide results comparable to those of tire tests.

As far as possible, the results have been related to the experiences gained with tires. The testing device used was developed by the firms Metzeler and Dix. Kern[4] considers three test procedures. One, which suggests testing until break occurs, requires much time and gives results of a wide statistical range. The second method, measuring time up to a predetermined residual strength, is regarded to correspond most closely to actual service conditions. Another, third procedure suggested by Kern employing a certain number of flex cycles for testing the residual strength has here been adopted.

It has been found advantageous to demonstrate

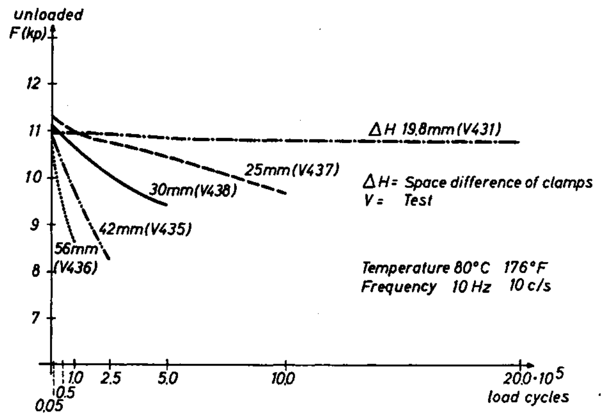

Fig. 1. Residual strength as function of the load cycles at different flex angles and amplitudes.

the strength variations through a number of load cycles as a sort of Wöhler curve rather than recording just two points like the strength before and after a given stress. The coefficient of variation for each measured point amounts to 2.5–6%. Assuming 95% probability, the limit of confidence of all estimated points is in most cases about 100 g. or 1%, since each one of the readings represents the arithmetic mean of 50 single measurements of cord sample strength.

To a certain extent any laboratory test must depart from reality, in order to measure various effects separately and to exaggerate testing conditions for faster and likewise more economical results. Nevertheless, the test conditions should resemble actual service treatment or at least maintain a marked correlation with tire test results. Therefore the testing frequency of 10 cycles/sec. was chosen corresponding to the rotation frequency of a VW wheel at 60 km./hr. (37.5 mph). According to measurements by Kern, the compression stress exceeds the constant tensile stress caused by the inflation pressure only for a quarter revolution of the tire. The testing frequency of 10 cycles/sec. refers to the time of one wheel rotation. The temperature was kept constant at 80°C. (144°F.) by means of a thermostat.

1.2 Effects of Pulsator Amplitude and Flex Angle on the Residual Strength

Effects of pulsator amplitude and flex angle on the residual strength of 1650/2 improved cord, twist 12.3/12.3 tpi, were studied at 144°F. and 10 cycles/sec. Variations of the flex angle or pulsator clamp amplitude differences of 20 to 56 mm. cause alterations in strength performance, as shown in relation to the flex ratio in Figure 1. With increasing amplitude the strength declines rapidly. An amplitude difference of 20 mm. cuts down strength by 5% after only 10^5 load cycles. This amounts to a loss of strength equal to that found with the same cord type in the innermost ply of a passenger car tire after approximately 50.000 km. (31,069 miles). Thus terms are found for a comparison with the residual strength of De Mattia cord samples and of the first tire samples, all of which were subjected to a similar stress. The tests were continued through one or even two million load cycles, thus disclosing characteristical differences between cord samples which would appear only in this range and simulating the conditions of a tire tester.

1.3 Influence of Twist

The strength of improved cord 1650/2, was studied at an amplitude of 20 mm. (0.78 in.) at 144°F. German tire producers do not agree

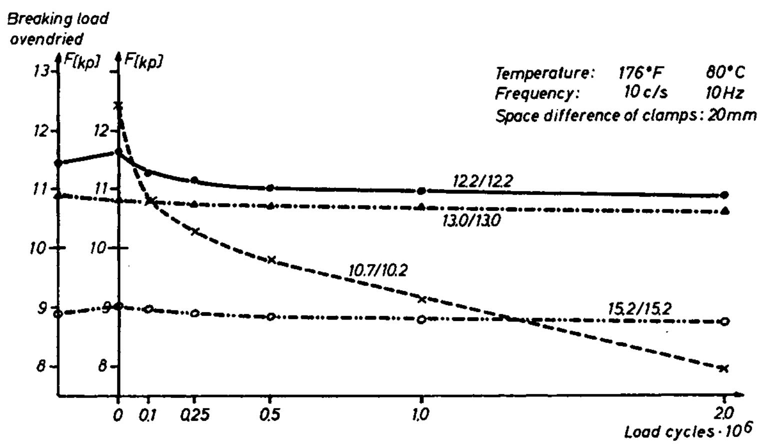

Fig 2. Effect of twist on compression fatigue (Wöhler curve).

unanimously on the twist giving best results. Some firms choose the symmetrical 12.3 Z 2× 12.3 S for Td 1650 yarns, others prefer 10.8 Z 2× 10.2 S. Kern[4] already pointed out the effect ply twist exerts on compression fatigue. He found that the yarn twist 10.8/10.2 tpi shows a steeper strength decline than yarns with a higher twist. Other in-rubber tests confirm this.[5,6]

Figure 2 shows the diminishing strength properties of yarns with twists of 10.8/10.2, 12.3/12.3, 13/13, and 15.3/15.3 tpi as related to the load cycles. Under the conditions chosen here, after 1.3×10^6 load cycles the yarn of twist 10.8/10.2 falls below all other yarns in strength readings. It is remarkable that in yarn 10.8/10.2 and similarly twist 12.3/12.3 tenacity at first drops almost exponentially until 10^5 load cycles are reached, whereafter there is a rather linear decrease of tensile strength. Higher twist yarns, however, show initially an almost rectilinear, parallel, and modest decline of tenacity.

At present investigations are still under way to determine the effect of twist on the compression fatigue together with other physical data. There is strong evidence that with increasing twist the residual strength is less sensitive to breaking of capillaries and that cord elasticity augments.[7]

For the evaluation of the test results the tenacities of yarns before flexing are compared with those after 10^6 load cycles as well as to the tenacity difference of 10^5 and 10^6 load cycles (Table I).

TABLE I
Summary of the Strength F of Various Cord Constructions before Flexing and after 10^6 Load Cycles, and the Drop in Strength ΔF after 10^6 Load Cycles or between 10^5 and 10^6 Cycles

Cord construction Z/S, tpi	Strength F, kiloponds		ΔF, %	
	Before flexing	After flexing 10^6 cycles	After 10^6 cycles	Between 10^5 and 10^6 cycles
10.8/10.2	12.42	9.1	26	15.0
12.3/12.3	11.64	11.0	5.5	3.3
13.0/13.0	10.8	10.7	1	0.8
15.3/15.3	9.0	8.8	2.2	2.0

Accordingly the 13/13 tpi yarn, which shows a high initial tenacity with hardly any subsequent loss, seems to be superior to all the other yarns. This is illustrated even better in Figure 3, summarizing the relation of twist and tenacity with the dynamic stress levels as parameters. Obviously the symmetrical twist 12.4/12.4 reaches its peak tenac-

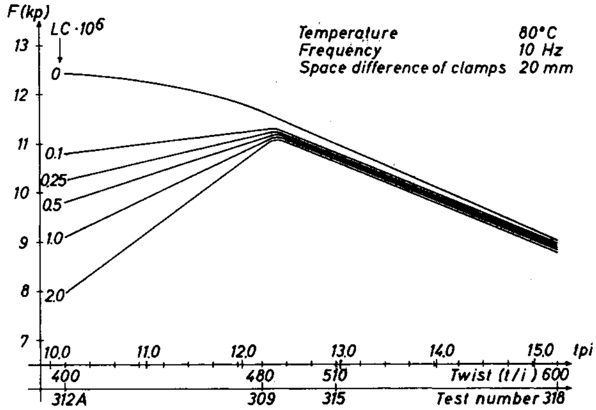

Fig. 3. Effect of twist on compression fatigue (F vs. Z plot).

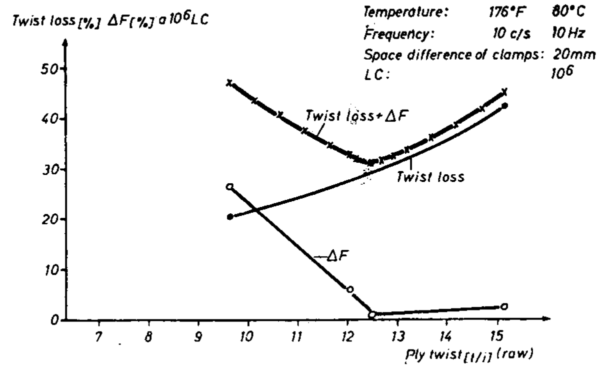

Fig. 4. Twist loss ZV and compression fatigue ΔF.

ity already after the application of little dynamic stress. A decrease of the static tenacity[8,9] may serve to explain the residual strength optimum, i.e., greater twist loss ZV—the complement of the cord yield to 100%—and increasing compression resistance, which indicates smaller tenacity loss with higher twist (Fig. 4).

According to Figure 4, the twist loss ZV of the dipped improved cord rises almost linearly from 20% for 10.2 tpi ply twist to approximately 40% for the 15.3 tpi twist. According to the residual strength curve in Figure 3, a minimum total tenacity loss is encountered at about 12.6 tpi. This minimum of tenacity loss corresponds to the optimum of the residual strength at a certain twist; it is the sum of tenacity loss ZV and compression fatigue ΔF.

This twist—12.6/12.6 tpi—found to give optimum residual strength permits the drawing of an analogy to the results of tire road tests in the U. S. A. There tire cords with various yarn twists have been investigated to the effect that the 12/12 twist emerged with superior results.

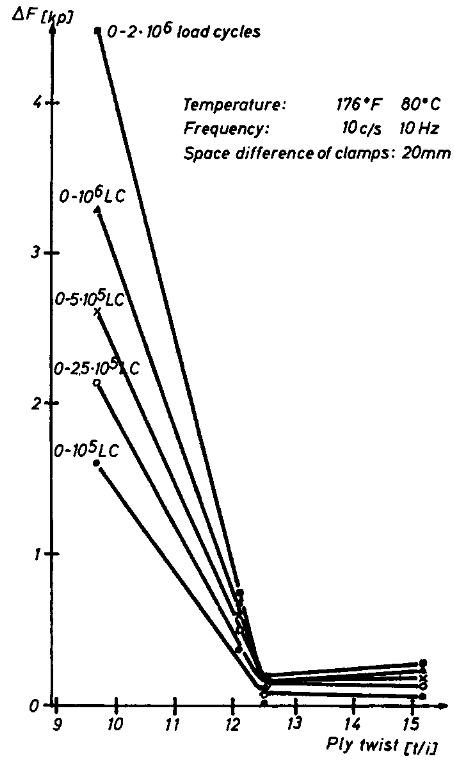

Fig. 5. Compression fatigue ΔF as function of the ply twist AZ.

The De Mattia test also provided results which resembled closely those obtained by German tire firms. A road test of 50,000 km. (31,069 miles) has demonstrated for the innermost ply of the tire with the same cord type a tenacity loss of 15% for 10.8/10.2 tpi and of 5% for 12.3/12.3 tpi twist in the flex region as opposed to the profile region. The De

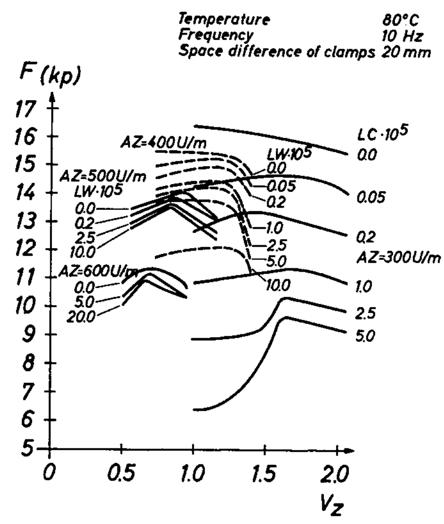

Fig. 7. Influence of twist ratio V_Z on the residual strength after various load cycles.

Mattia test shows an analogous drop of strength after 100,000 load cycles at an amplitude of 0.78 in. From this it may be concluded that there is no substantial increase of tenacity loss from twist 13/13 tip on upwards at increasing twist and stress (see Fig. 5).

Figure 6 attempts to determine the strength of a symmetrical twisted yarn after a certain number of flex cycles. If a parallel to this result can be drawn for actual tire performance, the residual strength of the cord after a certain milage could be predetermined in this manner under conditions which would closely correspond to those chosen for the diagram.

Figure 7 shows the effect of ply and cable twist on the dynamic compression fatigue. Strength in

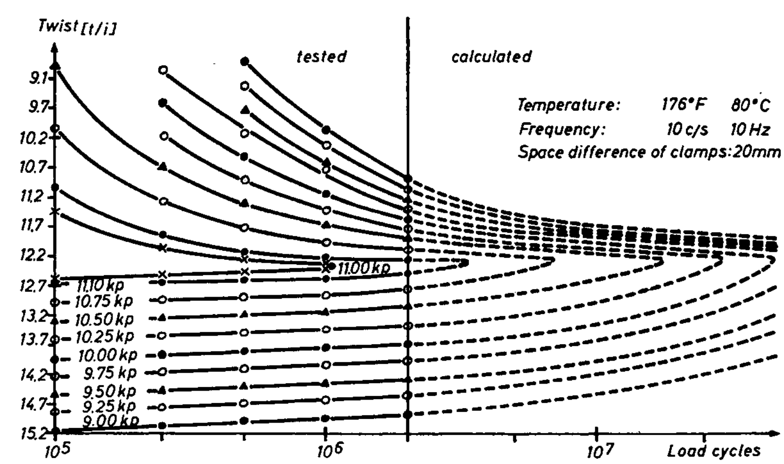

Fig. 6. Cable twist vs. load cycle plot with the residual strength as parameter; 1650/2 viscose improved cord.

kiloponds (kp.) is related to load. The 7.7 tpi yarn with greatest initial strength shows under increasing dynamic stress the largest loss of strength as compared to the cable twist series 10.2, 12.8, and 15.3 tpi. The test of this yarn had to be stopped after 500,000 load cycles, whereas tests of the other yarns were allowed to continue up to one or two million load cycles. Also the 10.2 tpi yarn values show a marked drop, while those for 12.8 and 15.3 tpi yarns drop insignificantly. The influence of the ply twist depends on the cord twist. While the optimum of the static strength of the 7.7 tpi ply twist lies below the yarn ratio $V_Z = 0.8$, i.e., below twist of 5.1/7.7 tpi, the peak strength after 10^5 load cycles occurs at $V_Z = 1.6$, i.e., at approximately 12.8 Z/2 × 7.7 S. The optimum strength of the cable twist 10.2 tpi shifts similarly from $V_Z = 0.8$ in the static test after 10^6 load cycles to $V_Z = 1.1$, i.e., to approximately 11.3 Z/2 × 10.2 tpi. At a cable twist of 12.8 the static and dynamic tests give equal values for optimal V, whereas with 15.3 tpi, the optimal V for dynamic testing falls below that for the static test. Conclusively, there is no steady strength optimum for yarns twisted below 12.8/12.8 tpi; increasing fatigue requires mounting V_Z values. Only from 12.8 tpi on up does the yarn maintain a stable optimal strength. Table II summarizes the strength optimum figures as related to the twist ratios.

TABLE II
Twist Ratio V_Z of Ply and Cord Twist and the Cord Construction for Optimal Strength after Compression Fatigue. The Twist Data Refer to Dipped Cord prior to Imbedding into Rubber

Ply twist, tpi	7.4	9.9	12.8	15.8
Flex cycles	5×10^5	1×10^6	1×10^6	2×10^6
Ratio of cord to ply twist Vz	1.65	1.2	0.85	0.65
Cord construction Z/S, tpi	12.2/7.4	11.7/9.9	10.9/12.8	10.2/15.8

The correlation of these findings with the elastic properties of cord is still subject to investigation. Savings of tire cord should be accomplished, however, if the optimal dynamic strength performances

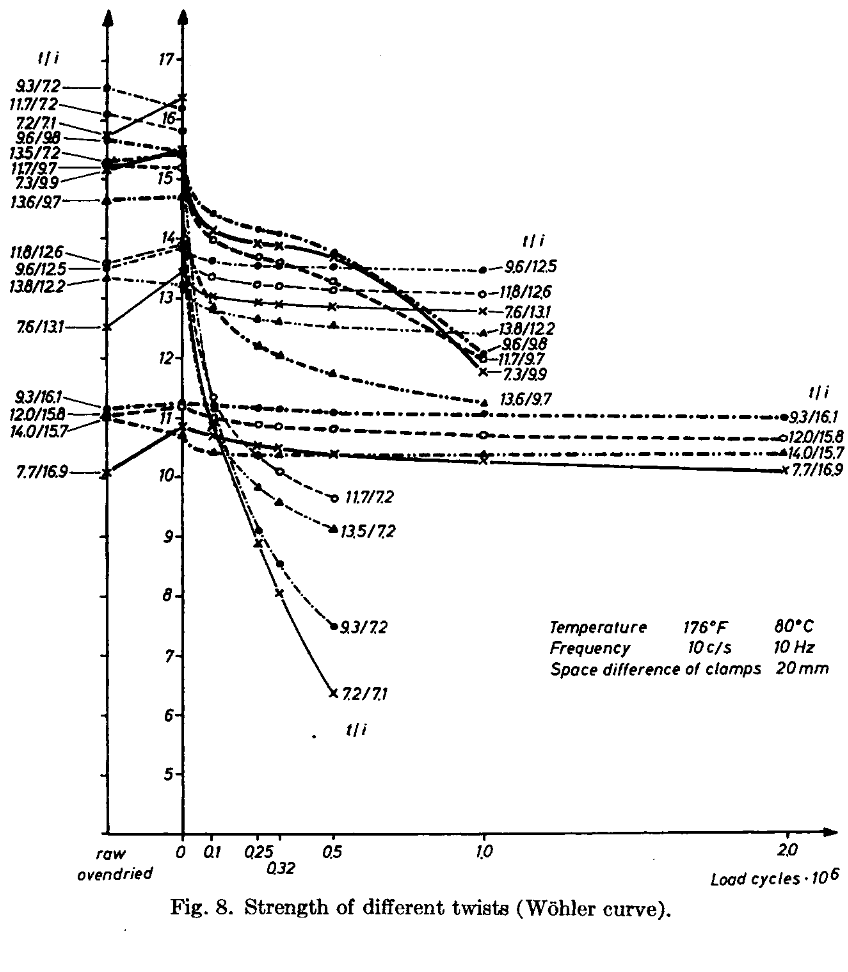

Fig. 8. Strength of different twists (Wöhler curve).

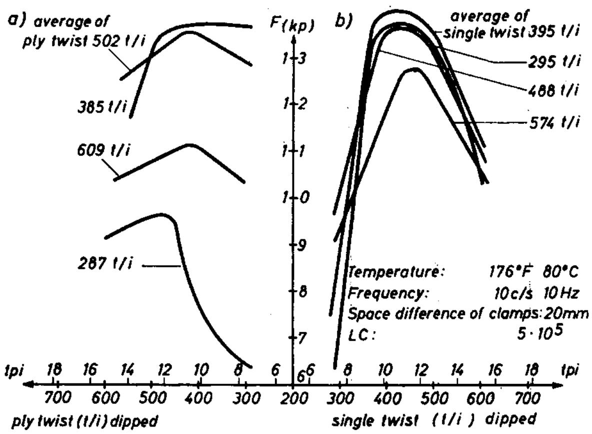

Fig. 9. Fatigue and twist construction.

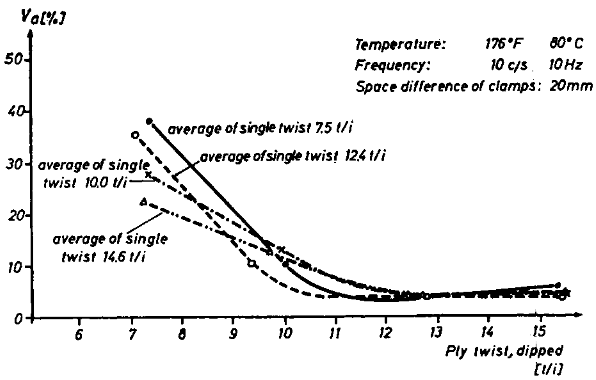

Fig. 10. Coefficient of variation V_a in dependence upon the ply twist.

of certain cord construction are considered. Figure 8 shows the Wöhler curves of the 16 cords.

Figure 9 demonstrates that the cord performance is more affected by the cord twist than by the ply twist. For this tested cord a twist of 11.5 tpi proved best, independently of the ply twist. This explains the optimal ply to cord twist ratio V_Z in Figure 7 and Table II.

With respect to the scattering (statistical range) of the experimental results, in Figure 10 the coefficient of variation V_a is plotted with the ply twist as parameter against the cord twist for residual strength of the various cords after 5×10^5 load cycles. Accordingly, the V_a of almost 40% for the 7.7 tpi cord twist is highest at the lowest ply twist of 7.6 tpi. V_a drops to 22.5% with 7.7 tpi at increasing ply twist up to 14.7 tpi. The V_a coefficient decreases still more—down to 5% at 11.5 tpi—with rising cord twist and remains then constant to 15.3 tpi for all ply twist. Therefore, it will have a favorable effect on residual strength uniformity after flexing to use yarns of the tested super cord with a ply twist not below 11.5 tpi.

1.4 Influence of Denier

The influence of denier on strength was studied at 0.78 in. amplitude, 144°F., 10 cycles/sec.

1.41. Influence of Cord Denier at Equal Single Denier of the Capillaries. Figure 11 compares the compression fatigue of two different deniers of a viscose-improved cord (Td 1650 and 1100). Here the strengths are plotted relatively in Rkm or grams per denier (Rkm = Reisskilometer = 9 × g./den.) and the cord twist of symmetric yarn as cord coefficient α_Z, where the cord coefficient $\alpha_Z = t\sqrt{T/9000}$ (t = tpi and T = denier) is the twist of Td 9000 cord (compare Deutsche Normen 1957, DIN 55 832). In order to compare the performance of different cord deniers, the strength in Rkm

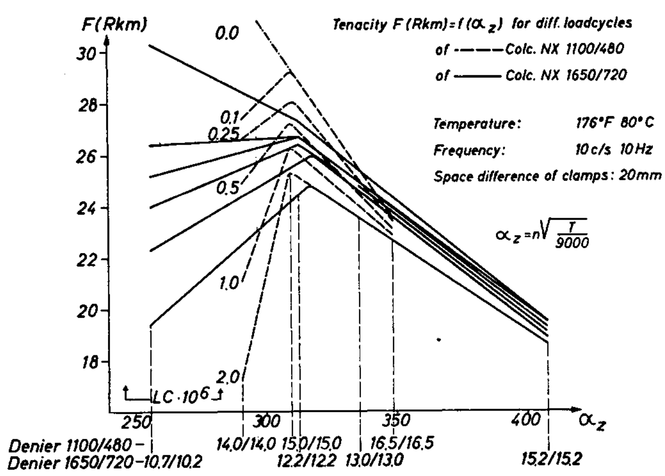

Fig. 11. Influence of yarn denier on compression fatigue: F vs. α_Z plot.

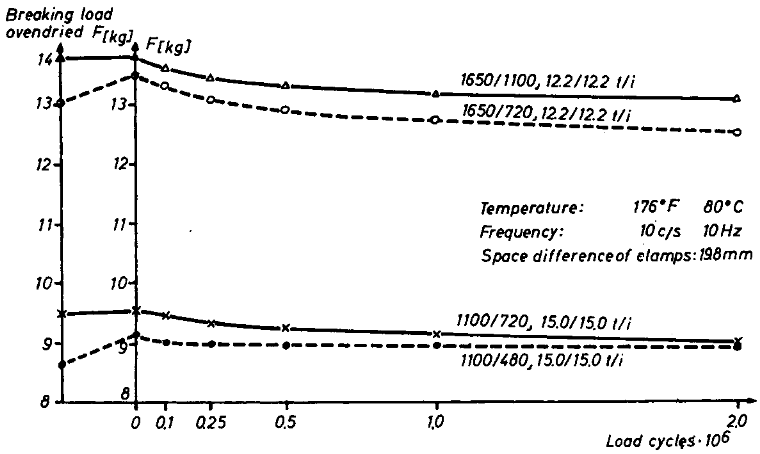

Fig. 12. Influence of the single denier on compression fatigue, residual strength as function of the load cycles (Wöhler curve).

represents a function of the coefficient α_Z, i.e., the cord twist as expressed for 9000 den. Both series of curves for 1650 and 1100 den. cord, are similar. The curves of 1100 den. cord, however, decline much more steeply from the vertex to lower α_Z values than those for 1650 den. cord.

The vertex of Td 1100 lies at an α_Z of 310, i.e., at the twist 15.13/15.13, whereas that of Td 1650 den. lies between α_Z 313–319, i.e., at approximately 12.4/12.4 tpi. From this could be expected that tires with 1100/2 fabrics of twists below 15.13/15.13 tpi would have poorer performance than higher twist fabrics. This has been confirmed by tire tests.

1.42. Influence of the Single Denier of the Capillaries at the Same Cord Denier. In Figure 12 the compression fatigue of viscose super cords with 1650 and 1100 den. and with the single deniers 2.3 and 1.5 den. (1650/1100 and 1100/720) is tested. The cord twist for 1650 den. was 12.3 tpi and for 1100

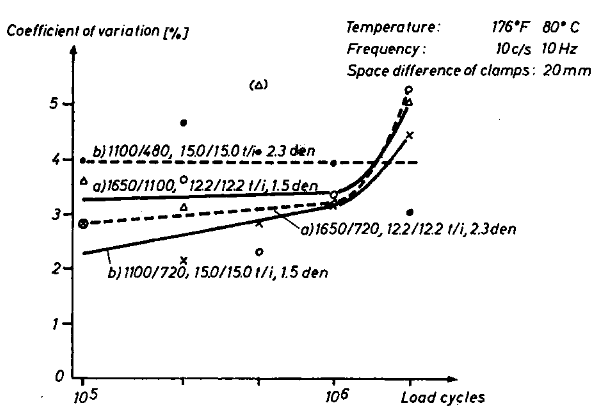

Fig. 13. Influence of single denier on coefficient of variation.

den 15.13 tpi. The higher static initial strength of 14 kp. for raw cord 1650/1100/2 with the finer single denier diminishes in dipping processes. This strength after dipping, however, remains in the residual strength after dynamic stress, i.e., the relative decrease of strength of 5.3% for finer single denier is somewhat smaller than that for the coarser one (7.7%). For the 1100/720/2 cord the initially higher strength as compared with the coarser single denier 1100/480/2 declines a little faster; after 2×10^6 load cycles both have the same residual strength.

The uniformity of the test results as expressed by the coefficient of variation is especially good for the 1100/720 single denier 1.5 (Fig. 13).

The dipping process may have further effects. Evidently the performance of the finer single denier is superior to that of the coarser ones regarding compression fatigue. This advantage is especially marked at lower load cycles, i.e., smaller compression fatigue as occurring under normal service conditions on the road.

1.5 Influence of Dip

Kern[4] has studied the influence of dip distribution (the quantity absorbed) on the compression fatigue and found that too "thick" an impregnation can lead to a greater compression fatigue. The two present test series compare compression fatigue with two different dip agents A (resonin paramaldehyde latex) and B (regenerated latex), at about the same amount (5%) of impregnation on a 1100/2 fiber at an amplitude of 20 mm. (0.78 in.) at 144°F., 10 cycles/sec.

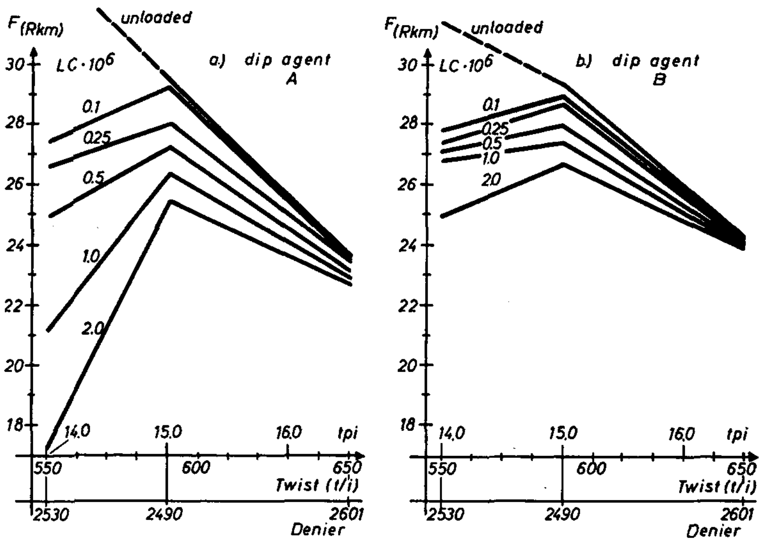

Fig. 14. Influence of dipping agent on compression fatigue.

The curve of strength of these cords related to the cord twist in Figure 14 is similar to that in Figure 3. At a cord twist of 15.13 tpi a strength optimum for both dip agents is observed. The strength of cord treated with agent A, however, is altogether somewhat lower than after impregnation with agent B. In addition, use of dip B yields better fatigue resistance than use of dip A. The optimal strength values after 2×10^6 load cycles and at a 15.13 tpi twist for B-treated cord are approximately 1 kp. higher.

Figure 15 illustrates the residual strength slope of the De Mattia cord samples with the flex cycle parameter as function of shrinking or stretching in the dipping process. According to the diagram, stretching during dip seems to have a better effect on compression fatigue resistance than shrinkage.

In Figures 16 and 17 the slope of the total strength loss for one cord is investigated. Figure 16 demonstrates the effect of load cycles on cord lengths not altered in dipping and Figure 17 on shrinkage of 2%. Various resorcin–formaldehyde solutions were also employed. The absorption of dipping agent was almost constant for both tests.

For dip test A (Fig. 16) the decrease of cord strength after 5×10^5 load cycles with rising twist shows a steeper slope than the loss of strength in dip test B (Fig. 17). Up to 9.3 tpi A loses very little strength at higher twist, whereas for test B from 11.3 tpi on a small and gradual loss of strength is observed.

Comparison of almost symmetrical cords at an increasing number of load cycles shows that in all cases a shift of the minimum strength loss ΔF to

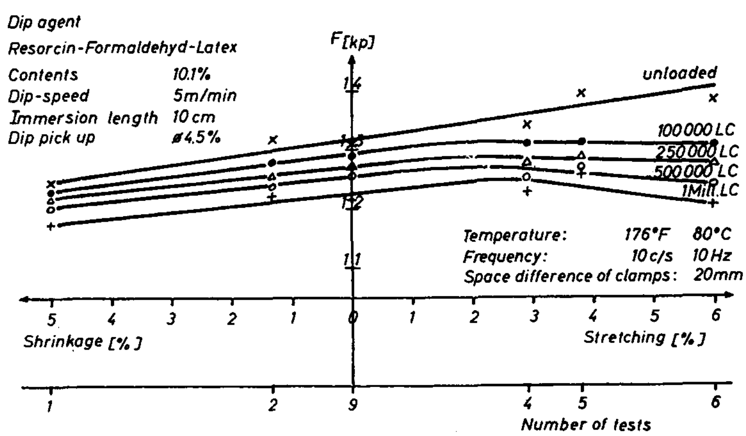

Fig. 15. Influence of stretch and shrinkage of twist in dipping on compression fatigue.

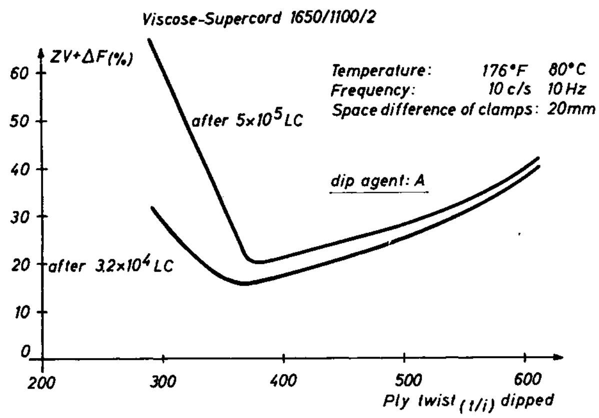

Fig. 16. Correlation between twist loss (ZV) + fatigue (ΔF) and ply twist, with load cycles.

higher twists has occurred, corresponding to a shift of the optimal cord strength. In test A the minimal loss of strength changes from 9.2 tpi after 3.2×10^4 load cycles to about 9.6 tpi after 5×10^5 load cycles; in test B the shift is from 10.3 tpi after 3.2×10^5 load cycles to 11.5 tpi after 5×10^5 load cycles.

The conclusion can be drawn from this that dipping processes substantially influence the compression fatigue of tire cords. According to former results and data now available the following factors have a marked effect: (*1*) the chemical composition of the dip agent; (*2*) the distribution of the agent in the cord; (*3*) shrinkage or stretching in the dip.

Influence of Temperature

The influence of temperature was studied at 20 mm., 10 cycles/sec.

1.61. Influence of Temperature on the Compression Fatigue of Viscose Cords. The development of cars with high speed performance and partly smaller tires has caused the average temperatures in the tires to rise. Therefore, the influence of the temperature on compression fatigue is of importance. Figure 18 compares test results optained with a viscose super super, a viscose super, and a viscose improved cord; the twist for all three 1650/2 types is 480/480. Up to 120°C., and after 2×10^6 load cycles the viscose improved cord does not show any substantial reduction of strength. This test had to be discontinued at 150°C., because the supporting rubber for the test specimen broke. On account of the uniform strength slope, however, it was possible to extrapolate the values for the improved cord up to 500,000 load cycles. The strength values of the viscose super cord exceed those of the improved type by approximately 3 kp. at 80°C., but decline with higher temperatures more rapidly. The strength of the super super cord is initially about 2 kp. higher than that of viscose super; it is, however, already decreasing at 80°C. and thereafter drops rapidly with rising temperatures and load cycles.

1.62. Influence of Temperature on the Compression Fatigue of Nylon Cord. Two nylon cords, I and II, are compared in Figure 19. The nylon improved cord I shows a higher compression fatigue than the number II cord in all temperature ranges. Its strength, initially higher by 1 kp., drops with increasing load cycles and at 80°C. after 10^6 load cycles is at the same level as that of the nylon cord II. At 100°C. the strength of cord I is inferior to that of nylon cord II after 250,000 cycles, and at 120°C. the strength drops below that of cord II after only 7,000 load cycles.

1.63. Influence of Temperature and Humidity

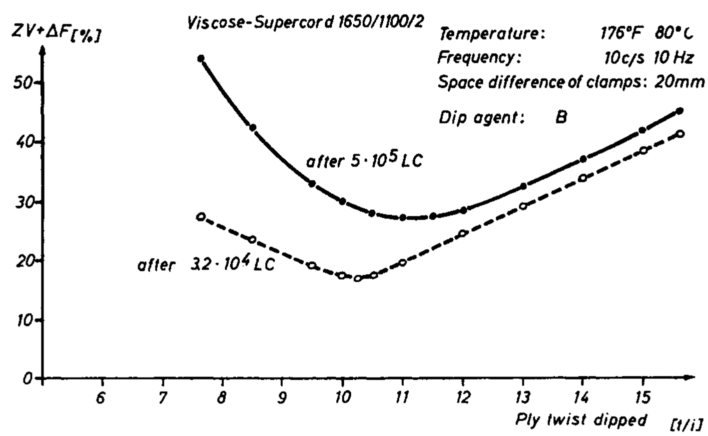

Fig. 17. Sum of loss in strength consisting of the compression fatigue ΔF and twist loss ZV as function of the cable twist.

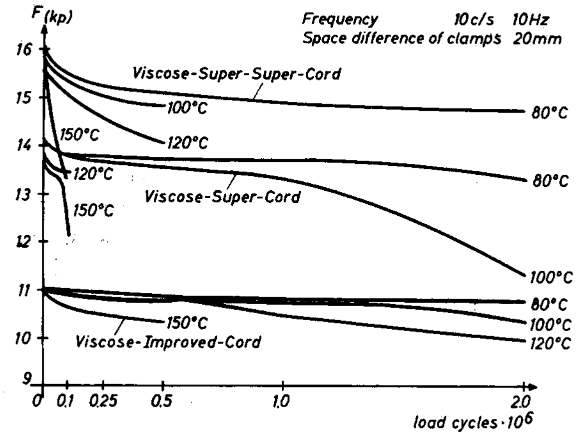

Fig. 18. Influence of temperature on compression fatigue of viscose cords.

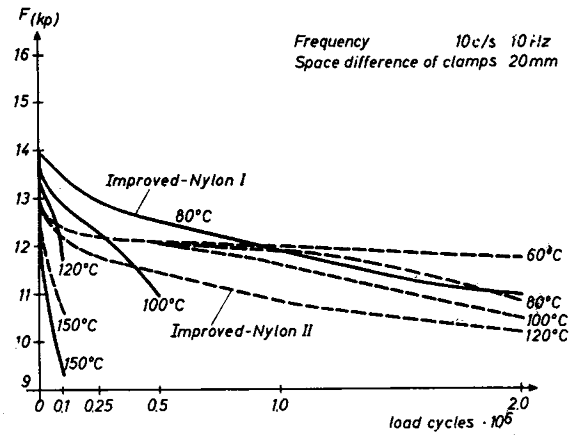

Fig. 19. Influence of temperature on compression fatigue of nylon cords.

Variations on the Test Results. During various tests the humidity, in conjunction with the temperature, has been observed as an undesirable secondary influence. During the tests performed a first without a thermostat the temperature at night dropped to 14°C. at relative humidity of 100% and rose for the day to 40°C. at 30% R.H. The residual strength of cord samples stressed at night was several kiloponds lower than that of the samples tested at daytime with higher temperatures.

1.7. *Influence of Frequency*

The influence of frequency was studied at 80°C. with 20 and 56 mm. space between the clamps. Figure 20 shows the range of the influence the frequency exerts on the compression fatigue. According to the graph there is no influence of frequency under mild conditions, i.e., a temperature of 80°C. and an amplitude of 20 mm. All three test series with the frequency 5, 10, and 25 cycles/sec. came up with the same residual strength. This changes, however, with increasing amplitude; with a higher amplitude the values for residual strength are higher at 25 cycles/sec. than at 10 and 5 cycles/sec.

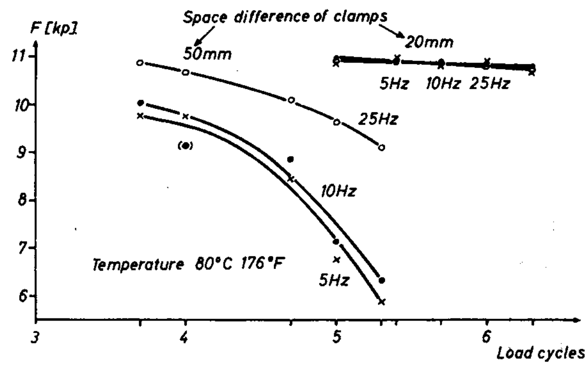

Fig. 20. Influence of frequency on compression fatigue.

This is demonstrated in Figure 21, where the residual strength is plotted against the amplitude with the frequency as parameter. To this time no corresponding conditions in tire use are known. Similar results have, however, been obtained in damping, as for instance with the Meskat-Rosenberg-Hoffmann apparatus (see below). No effect of the frequency on the bending angle of the flexing zone could be found with stroboscopic examinations.

Especially with regard to results of the Meskat-Rosenberg-Hoffmann instrument it is evident that the influence of the frequency in dynamic stress of cords is mainly observable in the external friction of the fibers, i.e., the friction between the single capillaries (see below).

The hardness of the supporting rubber—for tires the sidewall—enters the test results when the same carcass rubber is used in such a way as to give a small loss of strength with softer rubber.

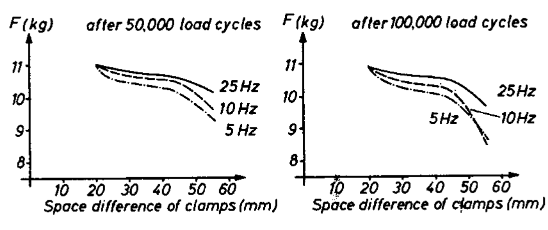

Fig. 21. Influence of the flex angle (amplitude) on the residual strength at various frequencies.

1.8. Influence of Cord Type

It is impossible to give a complete account of all the effects the manufacturing process may have on the compression fatigue. Research still is in progress in this field. The best way to show the influence originating in manufacturing processes is to compare various cord types made from different pulps and spun according to several methods.

Figure 22, for instance, is a comparison of two viscose improved cords with two viscose super cords 1650/2, 480/480. The space between the clamps was 56 mm. for this test, the frequency 10 cycles/sec., and the room temperature 30°C. Due to the big amplitude all types suffered a great

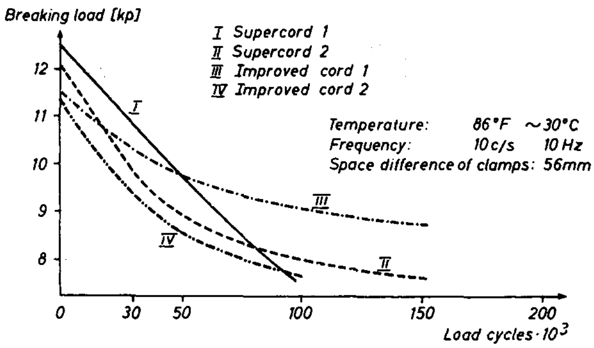

Fig. 22. Residual strength as function of the load cycles: Wöhler curve.

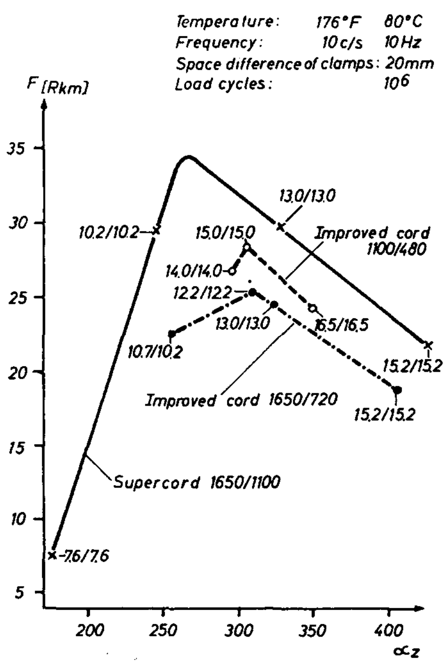

Fig. 23. Compression fatigue of a viscose super cord, 1650/2 and two viscose improved cords, 1650/2 and 1100/2.

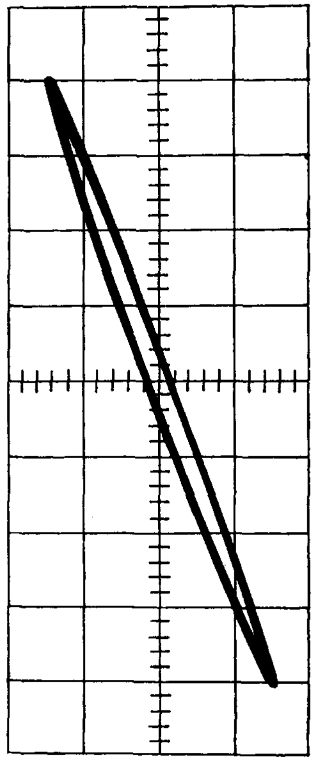

Fig. 24. Hysteresis loop of 1650/2 viscose super cord.

loss of strength. The extreme is only the strength slope of the super type C, 1, which shows a much steeper decline than any other type. This cord is said to have failed in tire service. The other three cords have been successfully used for high performance tires. The indoor wheel test of improved cord III, 1, gave extraordinary results, as confirmed by De Mattia results superior to the rest. Here also, a correlation is obvious between laboratory testing and indoor wheel tests.

In Figure 23 the slope of strength of a viscose super cord 1650/2 is related to the strength characteristics of viscose improved cords 1650/2 and 1100/2 after 10^6 load cycles in the strength F cord coefficient α_Z diagram. The strength curves for symmetrical yarns of these types vary widely. The optimum strength of the improved cord 1650/2 is reached at the twist 480/480, that of 1100/2 at 590/590, and that of viscose super cord at twist 410/410. Actually the super cord strength drops from the vertex towards lower twists (smaller α_Z) four times more steeply than to higher twists (greater α_Z). The tenacity curves of cords twisted above 500/500 all run parallel, the super cord maintaining a strength 0.55 g./den. higher than that of the improved 1650/2. Hence super cords can be processed with less twist than improved cords. The effects on compression fatigue, however, are with this cord, when twisted too low, considerably stronger than with improved cord. This has already been confirmed by indoor wheel tests.

2. Investigations on Growth and Damping of Tire Cords with the Meskat-Rosenberg-Hoffmann Apparatus

Several instruments have been developed for the examination of growth and damping on tire cords. Measurements have been made possible now in the field of resonance frequency[9] or audiofrequency and at very low frequency.[2,10,11] Miehlich[12] has investigated the influence of cord construction on damping at 50 cycles/sec. Similar studies have been made at 5 cycles/sec. by Breazeale and Whisnant.[13] Winkler[15] has given a detailed summary of these tests.

In the present paper the influence of frequencies from 0.5 to 50 cycles/sec. and the effects of the temperature on growth, inflexibility, and damping of various tire cords are shown.

2.1. Symbols Used

In Table III is given a list of symbols used for this discussion, as the proposal for the standardization of symbols for the dynamic units (quantities) is not yet available.

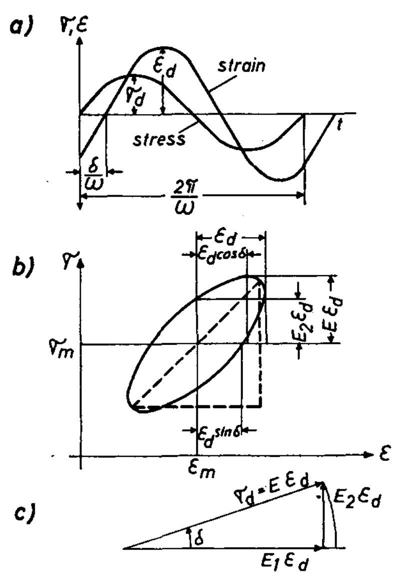

Fig. 25. (*a*) ϵ and τ as function of time; (*b*) hysteresis loop; (*c*) complex modulus *E*, Young modulus E_1; loss modulus E_2, and loss angle δ.

TABLE III

Symbol	Quantity	Units
M	Vibration mass per unit of length	pond/mm.
t	Time	sec.
ν	Frequency	sec.$^{-1}$
$\omega = 2\pi\nu$	Circle frequency	sec.$^{-1}$
l_0	Sample length at the start of the test	mm.
l	Sample length during the test	mm.
Δl	Length variation	mm.
Δl_V	Length variation effected by the initial load k_V	mm.
$l_V = l_0 + \Delta l_V$	Sample length under preload	mm.
Δl_d	Amplitude of length	mm.
k	Force (load)	kp.
k_d	Amplitude of force	kp.
ϵ	Elongation	%
ϵ_V	Preload elongation	%
ϵ_d	Amplitude of elongation	%
σ	Stress	kp./mm.^{2}
σ_V	Stress under preload	kp./mm.^{2}
σ_d	Amplitude of stress	kp./mm.^{2}
E	Complex modulus (inflexibility)	kp./mm.^{2}
E_1	Young modulus	kp./mm.^{2}
E_2	Loss modulus	kp./mm.^{2}
$H_{k,l}$	Hysteresis (loss energy)	mm.-kp., m.-kg., cal.
$H_{\sigma,\epsilon}$	Hysteresis (loss energy)	(kp./mm.^{2})
tan δ	Loss factor	
δ	Angle of loss	
b_k	Half width of the hysteresis loop parallel to the axis of load	kp.
b_l	Half width of the hysteresis loop parallel to the axis of length	mm.
q_0	Mass cross section of the unloaded sample	mm.^{2}
T_0	Denier of the unloaded sample	den.
γ	Specific gravity	pond/cm.^{3}
D	Damping	%
den	Weight/9000 m.	pond/m.

2.2. Correlation between Stress and Strain Assuming that Both Units Vary Sinusoidally

In many cases it can be assumed that the hysteresis loop resulting from the sinusoidal alternate strain on the cord sample tested is almost elliptically shaped. It follows that the alternate load shows an almost sinusoidal slope. The comparison of the planimetric area to that computed from the ellipse equation shows how far this holds true with the tests. On the basis of sinusoidal strain and stress conditions the following correlations are found according to Figure 25.[16,17]

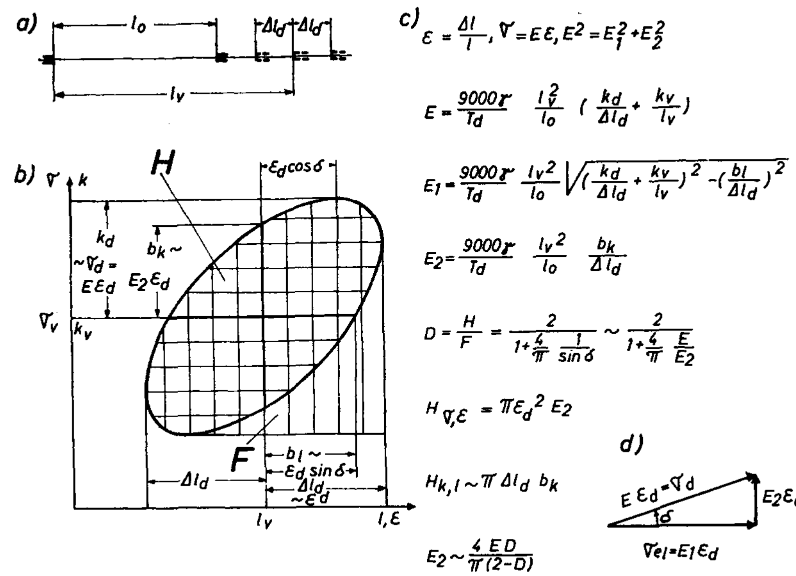

Fig. 26. Correlation between stress, strain, modulus, hysteresis, and damping.

$$M\ddot{\epsilon} + (E_2/\omega)\dot{\epsilon} + E_1\epsilon = \sigma_d \sin \omega t \quad (1)$$

The general solution of eq. (1) is:

$$\epsilon = \sigma_d \sin (\omega t - \varphi)/[(E_1 - M\omega^2)^2 + E_2{}^2]^{1/2} \quad (2)$$

The loss factor tan δ is, according to eq. (3) (Fig. 25*c*):

$$\tan \delta = E_2/E_1 \quad (3)$$

The angle φ of the eq. (2) is given as:

$$\tan \varphi = E^2/(E_1 - M\omega^2)$$
$$= \tan \delta/(1 - M\omega^2/E_1) \quad (4)$$

2.3. Preload Elongation, Complex Modulus, Young's Modulus, Viscosity Modulus, Specific Damping, and Loss Energy

Formulae for the growth ϵ_V in the preload k_V, for the complex modulus E, Young's modulus E_1, the viscosity modulus E_2, the specific damping D, and the loss energy H (Fig. 26) will be developed below.

Plastic stretch or change in length Δl_V effected by the initial length k_V results in preload elongation ϵ_V according to eq. (5):

$$\epsilon_V = (\Delta l_V/l_0)100 \quad (5)$$

Meskat's[10,18] complex modulus, which is also denoted as inflexibility, results from the ratio of stress to strain according to eq. (6):

$$\sigma = E\epsilon \quad (6)$$

This relation is a general one, which means that it can be applied to nonsinusoidal stress. Hence, it follows for the stress and strain amplitudes that

$$\sigma_d = E\epsilon_d \quad (6a)$$

If the stress and strain amplitudes of eq. (6a) are replaced by the force and length amplitudes and if the cross section q is computed from the denier T_0 of the unloaded sample the elongation E is, with regard to the change in the value for the cross section of the sample between the two points of the hysteresis loop reciprocal:

$$E = \left(\frac{9000\gamma}{T_0}\right)\left(\frac{l_V{}^2}{l_0}\right)\left(\frac{k_d}{l_d} + \frac{k_V}{l_V}\right) \quad (7)$$

The Young's modulus E_1 is, according to eq. (8):

$$E_1 = \left(\frac{9000\gamma}{T_0}\right)\left(\frac{l_V{}^2}{l_0}\right)\left[\left(\frac{k_d}{l_d} + \frac{k_V}{l_V}\right)^2 - \left(\frac{b_k}{l_d}\right)^2\right]^{1/2} \quad (8)$$

The loss or viscosity modulus E_2 follows from eq. (9):

$$E_2 = (9000\gamma/T_0)(l_V{}^2/l_0)(b_k/l_d) \quad (9)$$

According to Roelig,[19] the specific damping D is the ratio, expressed as percentage, of the loss energy H to the energy spent F (Fig. 19) as in eq. (10):

$$D = (H/F)100 \quad (10)$$

As eq. (10) is a general one, for an elliptic damping loop D can be computed according to eq. (11) (see Fig. 26) (compare Kainradl and Händler[17]):

$$D = 2\Big/\left(1 + \frac{4}{\pi}\frac{1}{\sin \delta}\right) \quad (11)$$

If $\sin \delta$ is replaced by the ratio of the half width of length b_l (Table III) to the amplitude of length l_a, the equation for D is:

$$D = 2\Big/\left(1 + \frac{4}{\pi}\frac{l_a}{b_l}\right) \quad (12)$$

Because

$$\sin \delta = E_2/E \quad (13)$$

it follows that

$$D = 2\Big/\left(1 + \frac{4E}{\pi E_2}\right) \quad (14)$$

According to Figure 26 the ratio E/E_2 equals the ratio of the load amplitude k_d to the half width of the hysteresis loop in the direction of force b_k. Hence, for the damping D:

$$D = 2\Big/\left(1 + \frac{4k_d}{\pi b_k}\right) \quad (15)$$

and for the modulus of viscosity E_2:

$$E_2 = 4ED/[\pi(2 - D)] \quad (16)$$

The hysteresis loop H, which is a measure for the loss energy, can be computed from the eqs. (17)–(24).

Hysteresis as lost energy, $H_{k,l}$, is

$$H_{k,l} = \pi \Delta l_d b_k \quad (17)$$

$$H_{k,l} = \pi k_d b_l \quad (18)$$

$$H_{k,l} = \pi \Delta l_d k_d E_2/E \quad (19)$$

Specific hysteresis brought into relation to the volume of the fiber, is given by

$$H_{\sigma,\epsilon} = \pi \epsilon_d E_2 \quad (20)$$

$$H_{\sigma,\epsilon} = \pi \epsilon_d \sigma_d E_2/E \quad (21)$$

$$H_{\sigma,\epsilon} = \pi \sigma_d^2 E_2/E^2 \quad (22)$$

$$H_{\sigma,\epsilon} = \Delta l_d b_k/l_0 q_0 \quad (23)$$

$$H_{\sigma,\epsilon} = (9000\gamma/T_0 l_0) l_d b_k \quad (24)$$

The choice of the suitable formula for the computation of the loss of energy depends on whether the constant amplitude of load, of elongation or of energy is used.

The lost energy as related to the volume will be determined with eqs. (20)–(24), whereas the eqs. (18) and (19) supply the data for the loss energy in m.-kp. With the help of these formulas planimetry can be avoided when the hysteresis loop is almost elliptically shaped or, when the loop can be depicted graphically by means of elliptic segments.[20]

2.4 Measurements

Previous measurements were performed together with W. Meskat and W. Hoffmann. The results shown here were obtained in cooperation with H. Meumann and W. Meskat.

2.41. Measuring Instrument and Process. Meskat and Rosenberg[10,14] have developed an instrument for load measurements with strain gages that can be applied to determine hysteresis, specific damping, and various elastic constants as well as

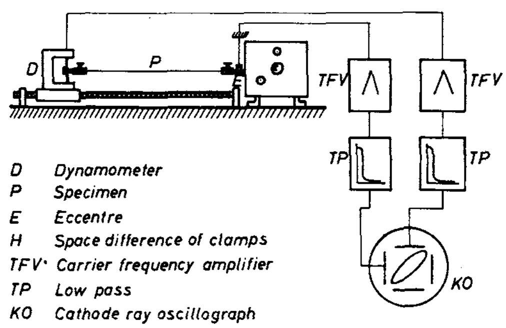

Fig. 27. Plot of the Meskat-Rosenberg-Hoffmann instrument.

the relaxation and retardation behavior and the degree of elasticity within the frequency range of 0.5–50 cycles/sec. This instrument has been further developed by W. Hoffmann and was used for the present investigations by H. Meumann. The load and elongation measurements were carried out with strain gages the deformations of which have been intensified on an oscillograph (Fig. 27).

2.5 Discussion of the Measurement Results

2.51. Elongation or Creep of Preloaded Cord. The elongation or creep of cord exposed to a preload weight $k_V = 1.5$ kp. at a temperature of 20°C., a frequency of 50 cycles/sec., and a constant elongation amplitude $\epsilon_d = 0.5\%$ was determined by use of eq. (5). The various cords in Table IV show differences in elongation. Viscose super cords stretch least, viscose improved cords stretch most, and the elongation of viscose super super cord lies between the two. This is said to correspond to experiences made with tires.

TABLE IV
Preload Elongation ϵ_V of Various Cord Types at 20°C. k_V = 1.5 kp., ϵ_d = 0.5%, ν = 50 cycles/sec.

Cord type	$\epsilon_V = (\Delta l_V/l_V)100$, %
Viscose, improved cord	5
Viscose, super cord 1	3.25
Viscose, super cord 2	2.5
Viscose, super super cord	4.5

2.52. Complex Modulus, Young's Modulus, and the Loss Modulus. The complex modulus E, the Young's modulus E_1, and the loss modulus E_2, were computed according to eqs. (7), (8), and (9). The values of the complex modulus E differ, apart from one viscose super cord, only slightly, as can be seen in Table V. A higher degree of inflexibility of one super cord has also been found in the tire.

The Young's modulus E_1 does hardly differ from the complex modulus. It is interesting to note that super super cords have the greatest loss modulus E_2, whereas improved cords have the smallest one.

TABLE V
Complex Modulus E, the Young Modulus E_1, and Loss Modulus E_2, Measured at 20°C., k_V = 1.5 kp., ϵ_d = 0.5%, ν = 50 cycles/sec.

Cord type	E, kp./mm.^{2}	E_1, kp./mm.^{2}	E_2, kp./mm.^{2}
Viscose, improved cord	753	751	48
Viscose, super cord 1	820	817	71
Viscose, super cord 2	727	720	58
Viscose, super super cord	742	737	84

2.53. Specific Damping D According to Roelig. Table VI shows a summary of damping values of various cord types which have been found by planimetry according to eq. (10).

TABLE VI
Damping D According to Roelig at 20°C., k_V = 1.5 kp., ϵ_d = 0.5%, ν = 50 cycles/sec.

Cord type	D, %
Viscose, improved cord	10.0
Viscose, super cord 1	13
Viscose, super cord 2	10.5
Viscose, super super cord	15

It is remarkable that the lowest value of damping is obtained from the viscose improved cord, whereas viscose super super cord has the highest damping, thus forming a parallel to the loss modulus (Table V).

2.54. Hysteresis Loss $H_{k,l}$. The hysteresis area was found by use of the planimeter. The behavior of viscose cords is quite different from that of nylon cords. At a temperature of 20°C. (see Table VII) nylon cord has the same hysteresis loss as viscose super cord, while viscose improved cord shows the smallest loss. There is hardly any change in the values of the viscose cords at 60°C., whereas the hysteresis loss of the nylon cord shows a threefold increase. The difference between the viscose super and the viscose improved cord of about 30% should lead to different temperatures in the tire during indoor wheel tests. This is confirmed by data from several tire firms, which state that the temperatures in some super cord tires are approximately 10% higher. Other viscose super cords show no higher hysteresis loss and, as a parallel, the temperature in the tires are no higher than those in improved cord tires. The behavior of nylon has also been confirmed by the indoor wheel test result, if the tire construction was equal to that of the viscose tire.

TABLE VII
Hysteresis Loss $H_{k,l}$ (Calculated) at 20 and 60°C., k_V = 1.5 kp., ϵ_d = 0.5 or 1.0%, ν = 50 cycles/sec.

Cord type	$H_{k,l}$, cal./p. At 20°C.	At 60°C.
Viscose, improved cord	0.55	0.6
Viscose, super cord	0.79	0.8
Nylon cord	0.72	2.2

2.56. Specific Damping D, of an Improved Cord in Dependence on the Frequency. The damping decreases with increasing frequency (Table VIII). All cord types show a corresponding behavior.

TABLE VIII
Specific Damping D According to Roelig at 20°C., k_V = 1.5 kp., ϵ_d = 0.5%

Frequency, sec.$^{-1}$	D, %
0.5	16.5
2	13.2
5	13.4
10	12.6
25	12.1
50	10.0

Hence it follows that, in order to get a complete survey of the damping conditions in the tire, measurements must be carried out at the corresponding frequencies of 25 cycles/sec. and more. A complete change in conditions can occur at extremely low frequencies of, say, $^1/_{40}$ cycle/sec. and less.

2.57. Measurement of the Degree of Elasticity. The degree of elasticity, i.e., the ratio of elastic to total elongation was 7.5 or, 18.7% for viscose super super cords and 11% for a super cord. The viscose super super cord with the lowest degree of elasticity is said to have extremely good properties.

3. Comparison of the Results of Both Testing Processes with One Another and with the Performance of the Cord in the Tire

3.1. Comparison of the Results of Both Testing Processes

In another discussion the influence of the ply/cord twist ratio V_Z of a viscose super cord on damping has been investigated.

Figures 28–30 show the slope of the damping D in dependence on the cord ratio V_Z with the cord twist as parameter.

In Figure 28 the damping D has been determined by planimetry and in Figure 29 by the ellipse formula, eq. (15). Apart from one value at 9.8 tpi and V_Z = 0.75, which is exceptional, the four measurement series give curves running through a minimum. This minimum is more distinct for damping values with a hysteresis loop area computed by the ellipse formula (Fig. 29).

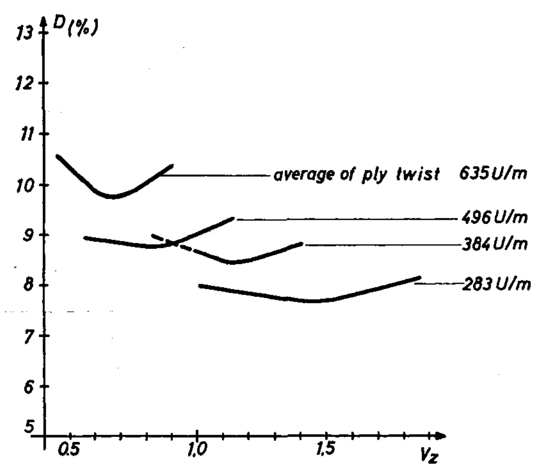

Fig. 28. Correlation between damping (%) and twist construction.

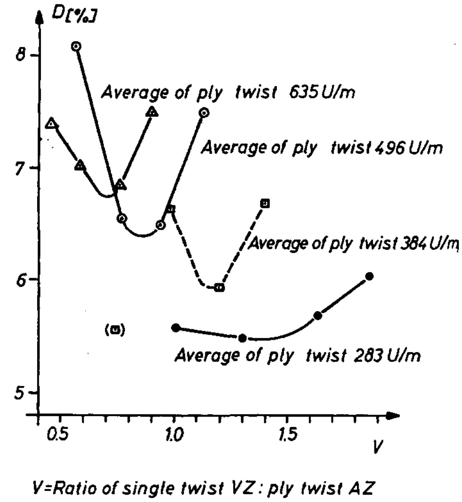

Fig. 29. Damping D of various viscose super cords.

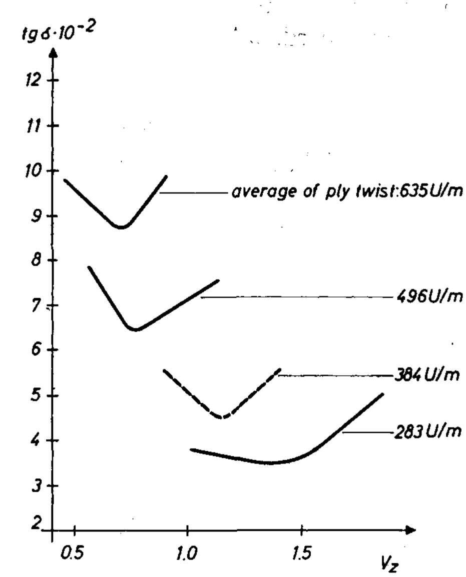

Fig. 30. Loss factor tan δ of viscose super cord.

The loss factor tan δ has a corresponding slope (Fig. 30). A comparison of the behavior of damping D or the angle of loss with the slope of the residual strength as obtained by the De Mattia test (see above, Fig. 8) shows that the minimum of damping or loss angle δ and the maximum residual strength after the De Mattia compression fatigue lie at approximately the same cord ratio V_Z (Table IX).

The loss ZV of oven-dried cord also shows a corresponding slope (Fig. 31). According to Table IX the minimum loss ZV, damping D, and loss factor tan δ of oven-dried cord appear at the same

TABLE IX
Ratio V_Z of the Ply Twist to the Cord Twist of a Viscose Super Cord 1650/2 having a Minimum of Damping *D*, of the Loss Factor tan δ and of the Oven-Dry Twist Loss *ZV*, Compared to the Maximum Residual Strength after Compression Fatigue According to De Mattia

	Minimum of damping *D*				
Cord twist, tpi	Plane geometric calculation, %	Computed, %	Minimum of loss factor tan δ	Maximum residual strength, kp.	Minimum twist loss *ZV*, %
7.25	1.4	1.35	1.4	1.4–1.6	1.4
9.8	(1.15)	(1.15)	(1.15)	1.15–1.2	1.05
12.7	0.85	0.85	0.75	0.93–0.83	0.83
16.2	0.65	0.73	0.7	0.7 –0.65	0.6

cord ratio *ZV* with the optimum residual strength after compression fatigue.

This permits a statistical correlation between three completely different testing methods: (*1*) the oven-dry static strength of raw cords; (*2*) the alternate tensile strength of raw cords as obtained in rubber tests on the Meskat-Rosenberg-Hoffman instrument; (*3*) the compression fatigue of imbedded rubber obtained according to De Mattia.

There are several correlations between the De Mattia compression fatigue of in-rubber tests and the results of tire tests.

The position of the single capillaries in the cord also influences the external friction and thus affects damping, compression fatigue, and static strength. The external friction seems to be an essential factor for cord fatigue. The extension of the internal friction still is subject to investigation. Evidently, the external friction does not only generate heat but also leads to the destruction of single capillaries, i.e., to so-called cord fatigue.

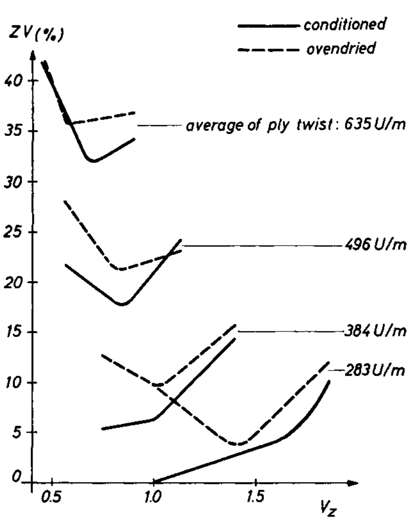

Fig. 31. Twist loss as function of the ply cable twist ratio V_Z for four different cable twists.

3.2. Comparison of the Results of the De Mattia Method with the Performance of the Cord in the Tire

In Table X the results from the compression fatigue obtained with the De Mattia method are compared with the performance of the cord in the tire.

A general correlation has been found for the following influences (Table X): (*1*) size of the flex angle; (*2*) cord twist; (*3*) single denier of the capillaries and cord denier; (*4*) dip; (*5*) cord type.

It may be assumed that extreme temperature conditions in the tire will have an effect in compliance with the test results.

The De Mattia method is not regarded as a universal test but rather as a method supplying information especially on the behavior of such tires which are expected to show considerable compression fatigue. Under normal conditions this test should be particularly informative for tires of scooters, motorcycles, passenger cars, and light trucks.

3.3. Comparison of the Results of Damping Measurements with the Behavior of Cord in the Tire

In Table XI the laboratory results obtained with the Meskat-Rosenberg-Hoffmann instrument have been compared to the behavior of tires.

The results of the Meskat-Rosenberg-Hoffmann testing method supply information on all types of tires, e.g., on giant tires as well as on passenger car tires.

Both testing methods—examinations of compression fatigue according to De Mattia as well as the investigations on the damping phenomena during alternate tensile stress by means of the Meskat-Rosenberg-Hoffmann instrument—show in several points a correlation with normal service conditions, e.g., with the indoor wheel test and with the road tests.

Furthermore, a correlation between both tests and with the static and tire test was noticed during investigations on the behavior of various cord constructions.

With the help of these two tests, tire firms can examine the changes to which cords are subiected

TABLE X
Comparison of the Flat Pad Test Results with Those of Tire Tests

Factor	Results obtained with the De Mattia instrument	Result of the tire test	Correlation[a]
1. Size of flex angle	Decreasing strength with increasing flex angle	Decreasing residual strength (decreasing life) with increasing flexing (decrease of inflation pressure)	+
2. Twist	Advantageous twist for improved cord 1650/2 486/486	Advantageous cord twist for 1650/2 472/472–510/510	+
3. Frequency	No influence under normal conditions		0
	Increasing destruction under severe flexing at decreasing frequency		0
4. Impregnation	B effects higher initial and residual strength than A	B effects higher initial and residual strength than A	+
5. Denier			
Cord denier	Td 1100 at least as good as Td 1650 if not better.	Td 1100 has proved good for the performance in the tire	+
Single denier	Finer single deniers show greater fatigue resistance on the average	Finer single deniers are preferred for use in the tire	+
6. Temperature	Increase in temperature does not effect an increase in the drop in strength of viscose improved cords		0
7. Cord type	Improved cords show a very low drop in strength	Tires manufactured from improved cord show a low drop in strength	+
	At a temperature of 80–100°C. viscose super cords show a higher strength than improved cords at strength ranges which are usual under normal service conditions	The gain in strength by the use of super cords partly causes advantages in construction	+
	One super cord showed compared to another super cord and to two improved cords bad results. One improved cord showed an excellent resistance to flexing fatigue.	The super cord type giving poor De Mattia test results showed low mileage during indoor wheel test; improved cord types with excellent De Mattia testing results reached high mileage	+

[a] Here + denotes positive correlation, − denotes negative correlations, 0 denotes no correlation known; parentheses indicate correlation is to indoor wheel test.

TABLE XI
Summary of Results Obtained with the Meskat-Rosenberg-Hoffmann Instrument

Measured values	Results obtained with the Meskat-Rosenberg-Hoffmann instrument	Behavior of the tire	Correlation[a]
Initial load elongation	Higher for viscose improved cord in comparison to super cord	Tires with improved cords show a higher growth than such with super cords	+
Inflexibility	A viscose super cord is more inflexible than other cord types	This result has been confirmed by the behavior of tires in service	+
Damping	Higher for viscose improved cord than for super cord		0
Hysteresis loss	Highest for nylon cord at temperatures above 40°C.		(+)
	Several viscose super cords show ca. 20% higher hysteresis loss compared to viscose improved cords	These viscose super cords are said to reach 10% higher temperature in the tire on the indoor wheel than improved cords	(+)

[a] Here + denotes positive correlation, − denotes negative correlation, 0 denotes no correlation known; parentheses indicate correlation is to indoor wheel test.

during the manufacturing process and they are enabled to choose from cords with different provenances those, which they consider most suitable for the use in the tire.

The manufacturers of tire cords can with these methods control their cord developments and study manufacturing and other influences on the compression fatigue of tire cords.

I thank the management of Glanzstoff-Courtaulds GmbH· for the permission to publish this report. Especially, I should like to express my thanks to Herr Dr. Domke, director of Glanzstoff-Courtaulds GmbH. for his promoting the work. Furthermore, I wish to thank Herr Espanion, Herr Körner, and Herr Kuhn who helped to carry out the investigations and to evaluate the results obtained.

References

1. Pieper, E., *Kautschuk u. Gummi*, **7**, WT148 (1954).
2. Fromandi, G., *Kautschuk u. Gummi*, **2**, 113 (1949).
3. Illingworth, J. W., *J. Textile Inst.*, **44**, 328 (1953).
4. Kern, W., *Kautschuk u. Gummi*, **8**, WT195, WT233 (1955).
5. Goy, R. S., *Proc. Rubber Technol. Conf., 3rd Conf., London*, 1954, "Cord fatigue testing."
6. Pieper, E., *Gummi u. Asbest*, **11**, 286, 500 (1958).
7. Keil, A., and S. Schulz, *Kautschuk u. Gummi*, **12**, WT-211 (1959).
8. Platt, M. M., *Textile Research J.*, **20**, 519, 665 (1950).
9. Kainradl, P., and F. Händler, *Kautschuk u. Gummi*, **8**, WT257, WT280 (1955).
10. Meskat, W., and O. Rosenberg, in H. A. Stuart, Ed., *Die Physik der Hochpolymeren*, Vol. IV, Springer, Berlin, 1956, p. 278.
11. Wegener, W., and W. Falch, *Reyon, Zellwolle u. Chemiefasern*, **35**, 542, 613 (1955).
12. Miehlich, W., *Reyon, Zellwolle u. Chemiefasern*, **32**, 412 (1952).
13. Breazeale, F., and J. Whisnant, *J. Appl. Phys.*, **20**, 621 (1949).
14. Kemmnitz, G., W. Meskat, and H. Meumann, *Rheologica Acta*, **1**, No. 2/3, 268 (1958).
15. Winkler, F., *Faserforsch. u. Textiltech.*, **9**, 109, 476 (1958); *ibid.*, **10**, 75 (1959).
16. Staverman, A. J., and F. Schwarzl, in H. A. Stuart, Ed., *Die Physik der Hochpolymeren*, Vol. IV, Springer, Berlin, 1956, p. 1.
17. Kainradl, P., and F. Händler, *Kautschuk u. Gummi*, **11**, WT193, WT222 (1958).
18. Meskat, W., and O. Rosenberg, *Reyon, Zellwolle u. Chemiefasern*, **31**, 555, 617 (1953).
19. Roelig, O. O., Deutsche Normen DIN 53 513, November 1944.
20. Kemmnitz, G., W. Meskat, und H. Meumann, *Rheologica Acta*, **1**, No. 2/3, 258 (1958).

Synopsis

The dynamical properties of tire yarns were investigated, the De Mattia method being used for compression fatigue and the Meskat-Rosenberg-Hoffmann instrument for the performance during an alternating tensile strength test. Various influences in the test of compression fatigue after De Mattia were investigated. The intensification of the test by increasing the flex angle leads to a considerable decline in tenacity. With increasing the ply twist, the residual strength shows a maximum which lies at an optimum of cord construction. The maximum of the residual strength follows from the increase of the static twist loss and the decrease of the compression fatigue according to the ply twist. The influence of dipping, temperature, and frequency as well as the properties of different cord types were examined. The correlation between tension and flexibility is shown during the alternating tensile strength test of raw cords assuming that both change sinusoidally. Equations for the calculation of the complex modulus, the Young modulus, and the viscosity modulus as well as of the specific damping and the loss energy are stated. Measurements were carried out with viscose improved and viscose super cords and some of the results compared to those for nylon cords. The damping shows in relation to the twist construction a minimum at a constant ply twist and at a certain cable twist which is represented by the ratio Vz of ply/cable twist. A comparison of the two dynamical test methods, i.e., the compression fatigue and the tensile strength test, shows that a maximum residual strength of a certain twist construction corresponds to a minimum in damping and in twist loss. So far there exists a correlation between the static and the two different dynamic tests. Finally, the results of the two dynamic test methods are compared with the properties of cords in the tire. This comparison shows that not even in one case do the results of the laboratory tests contradict the properties of cords in tires, but in most cases correspond to them. Therefore, it can be assumed that it is possible to investigate the dynamic properties of cord twists in tires by laboratory tests with both test methods, i.e., the compression fatigue after De Mattia and the loss energy with the Meskat-Rosenberg-Hoffmann instrument.

Résumé

On a étudié les propriétés dynamiques des fils de pneu par la méthode de De Mattia en mesurant la fatigue sous pression et avec l'appareil Meskat-Rosenberg-Hoffmann pour la performance au cours d'un test de force de tension alternative. On a examiné les différentes influences sur le test de fatigue sous compression d'après De Mattia. L'intensification du test au moyen d'une augmentation de l'angle de flexion conduit à une diminution considérable en ténacité. En augmentant la torsion du fil, la force résiduelle montre un maximum qui est lié à un optimum de construction du cordon. Le maximum de la force résiduelle résulte d'une augmentation de la perte de torsion statistique et du décroissement de la fatigue sous compression suivant la torsion imposée. De plus l'influence de l'immersion, la température, la fréquence aussi bein que les propriétés de différents types de cordons, ont été examinées durant ce test. On montre la corrélation entre la tension et la flexibilité pendant le test d'élongation alternative des cordes brutes en admettant que toutes deux varient sinusoïdalement. Les formules de calcul du module complexe, le module de Young et le module viscosimétrique, et de calcul de l'amortissement spécifique et de perte d'énergie sont mises au point. Les mesures ont été effectuées sur des fils de viscose améliorées et de superviscose et comparées, du moins en partie, aux fils en nylon. L'amortissement

montre en rapport avec la torsion un minimum à enroulement constant et pour une certaine valeur de celiu-ci qui est représenté par le rapport Vz de l'enroulement pli/cable. Une comparaison des deux méthodes de test dynamique, c.à.d. la fatigue sous compression et la force de tension, indique qu'une force résiduelle maximum correspond à un minimum d'amortissement et de perte d'enroulement. Ainsi il existe une corrélation entre le test statique et les deux test dynamiques différents. Finalement les résultats des deux méthodes de test dynamique sont comparés avec les propriétés des fils dans le pneu. La comparaison montre qu'en aucun cas les résultats de laboratoire ne sont contradictoires avec les propriétés des fils au sein des pneus, mais en général sont en bon accord. Ainsi on peut admettre qu'il est possible d'étudier les propriétés dynamiques des fils torsionnés dans les pneus au moyen de test de laboratoire par les deux méthodes indiqués, à savoir la fatigue sous compression suivant De Mattia et la perte d'énergie avec l'instrument de Meskat-Rosenberg-Hoffmann.

Zusammenfassung

Das dynamische Verhalten von Reifencorden wird sowohl mit der de Mattia-Methode auf Kompressions-ermüdung als auch mit dem Meskat-Rosenberg-Hoffmann-Gerät auf das Verhalten bei der Wechselzugbeanspruchung untersucht. Bei der Kompressionsermüdungsprüfung nach de Mattia werden verschiedene Einflüsse untersucht. Die Steigerung der Prüfintensität durch Vergrösserung des Knickwinkels führt zu einem starken Festigkeitsabfall. Bei einer Steigerung der Auszwirndrehung durchläuft die Restfestigkeit ein Maximum, das bei einer optimalen Zwirnkonstruktion liegt. Dieses Maximum der Restfestigkeit ergibt sich aus der Zunahme des statischen Zwirnverlustes und der Abnahme der Stauchermüdung mit der Auszwirndrehung. Weiterhin werden Einflüsse der Imprägnierung, der Temperatur und der Frequenz untersucht sowie das Verhalten verschiedener Cordprovenienzen bei der Prüfung. Bei der Wechselzugbeanspruchung der Rohcorde mit dem Meskat-Rosenberg-Hoffman-Gerät wird der Zusammenhang zwischen Spannung und Verformung unter der Annahme, dass sich beide sinusförmig verändern, dargestellt und Formeln für die Berechnung des komplexen Moduls, des Elastizitätsmoduls und des Viskositätsmoduls sowie der spezifischen Dämpfung und der Verlustenergie aufgestellt. Messungen sind mit Viskose-Improved- und -Super-Corden zum Teil im Vergleich zu Nyloncorden durchgeführt worden. Bei der Messung der Dämpfung in Abhängigkeit von der Zwirnkonstruktion ergibt sich bei konstanter Auszwirndrehung ein Minimum bei einer bestimmten Vorzwirndrehung, dargestellt durch das Verhältnis V_Z von der Vorzwirn- zur Auszwirndrehung. Bei einem Vergleich der beiden dynamischen Prüfverfahren, d.h. der Kompressionsermüdung und der Wechselzugbeanspruchung, zeigt sich, dass die maximale Restfestigkeit einer bestimmten Zwirnkonstruktion einem Minimum der Dämpfung und einem Minimum des Zwirnverlustes entspricht. Insofern besteht ein Zusammenhang zwischen der statischen und den zwei verschiedenen dynamischen Prüfungen. Zum Schluss werden die Ergebnisse der beiden dynamischen Prüfverfahren mit dem Verhalten des Cordes im Reifen verglichen. Dabei zeigt sich, dass in keinem Fall das Ergebnis der Laboratoriumsprüfung dem Verhalten des Cordes im Reifen widerspricht, sondern mit diesem in den meisten Fällen übereinstimmt. Deshalb wird es als möglich angesehen, mit diesen beiden Prüfverfahren, d.h. der Kompressionsermüdung nach der de Mattia-Methode und der Verlustenergiemessung mit dem Meskat-Rosenberg-Hoffmann-Gerät, das dynamische Verhalten des Cordzwirnes im Reifen bereits im Laboratorium weitgehendst zu untersuchen.

Received August 22, 1960